

# Search for a Light Higgs Boson at ATLAS

*Tatsuya Masubuchi on behalf of the ATLAS collaboration*

*International Center for Elementary Particle Physics, The University of Tokyo  
7-3-1 Hongo bunkyo-ku, Tokyo, JAPAN*

## 1 Introduction

The Higgs boson is predicted by the Standard Model (SM) as a natural explanation of the electroweak symmetry breaking that originates the mass of the  $W$  and  $Z$  bosons. Previous results from LEP, Tevatron and LHC had excluded the range up to 114.4 GeV and between 141 and 476 GeV [1, 2, 3]. Indirect limits of  $m_H < 158$  GeV at 95% confidence level (CL) have been set using global fits to precision electroweak results [4].

For the reasons mentioned above, the SM prefers the Higgs boson with relatively light mass. This note describes the results of search for a light mass Higgs boson using full data about  $5 \text{ fb}^{-1}$  collected in 2011 at  $\sqrt{s} = 7$  TeV with ATLAS detector[5].

## 2 Higgs boson search in the low mass region

The strategy of search for the Higgs boson depends on its production process and decay mode. The dominant Higgs boson production is via gluon-gluon fusion process, next vector-boson-fusion process and then the associated production with a  $W/Z$  boson. In the low mass region, the Higgs boson predominantly decays into  $b\bar{b}$  ( $m_H < 135$  GeV) and  $WW$  ( $m_H > 135$  GeV). While  $\gamma\gamma$ ,  $ZZ$  and  $\tau\tau$  decay modes are not dominant, these decay modes are also promising for the Higgs boson search since the final state can be selected requiring high  $p_T$  photons or leptons. In this section, the results of the Higgs boson search in the low mass region are described.

### 2.1 $H \rightarrow \gamma\gamma$ channel

The branching ratio of diphoton decay is very small, but a narrow Higgs mass peak can be observed over the background thanks to good photon energy resolution.

To optimize the sensitivity, the selected diphoton events are separated into nine mutually exclusive categories depending on whether the photon is converted or unconverted, the pseudorapidity of the photon and  $p_{Tt}$ <sup>1</sup>. This categorization extracts

<sup>1</sup> $p_{Tt} = |(\mathbf{p}_T^{\gamma_1} + \mathbf{p}_T^{\gamma_2}) \times (\mathbf{p}_T^{\gamma_1} - \mathbf{p}_T^{\gamma_2})| / |(\mathbf{p}_T^{\gamma_1} - \mathbf{p}_T^{\gamma_2})|$ , where  $\mathbf{p}_T^{\gamma_1}$  and  $\mathbf{p}_T^{\gamma_2}$  are the transverse momenta of the two photons



the region having better diphoton mass resolution and signal-to-background ratio, S/B. Finally, all nine categories are combined. The background model is obtained for each category by fitting diphoton invariant mass,  $m_{\gamma\gamma}$  in the range 100-160 GeV with an exponential function with free slope and normalization parameters. Figure 1(left) shows  $m_{\gamma\gamma}$  distribution summed over all categories. Figure 1(right) shows the observed and expected 95% CL upper limit on the cross section, divided by the SM prediction, as a function of Higgs boson mass. Two small regions, 113-115 GeV and 134.5-136 GeV are excluded. One interesting excess is observed around 126 GeV. The largest significance is  $2.8 \sigma$  at 126.5 GeV ( $1.5 \sigma$  when the look-elsewhere-effect in the interval 110-150 GeV is considered) [6].

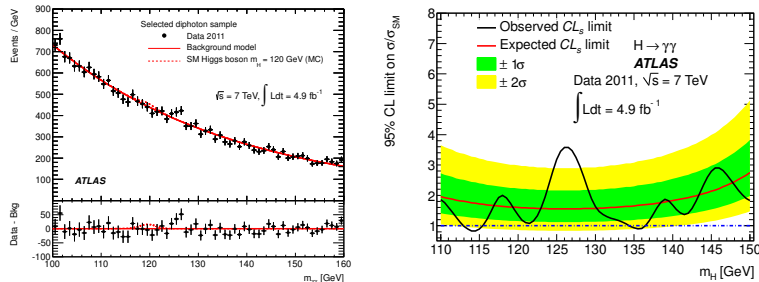


Figure 1: Left: diphoton mass distribution summed over all categories [6]. Solid line represents the background model fitted by an exponential function. Dashed line represents the signal shape of  $m_H = 120$  GeV. Right: The observed and expected 95% CL upper limit on the cross section, divided by the SM prediction, as a function of  $m_H$ .

## 2.2 $H \rightarrow ZZ \rightarrow 4\ell$ channel

This channel is very clean and provides good S/B thanks to the requirement of four isolated leptons ( $4e$ ,  $4\mu$  or  $2e2\mu$ ). The dominant backgrounds are non-resonant  $ZZ \rightarrow 4\ell$ ,  $Z$ +jets and  $t\bar{t}$  background in the low mass region. Four lepton invariant mass,  $m_{4\ell}$ , resolution is good (1-2%) and a narrow Higgs mass peak can be observed over a continuous background.

Figure 2 shows  $m_{4\ell}$  distribution (left) and the observed and expected 95% CL upper limit on the cross section, divided by the SM prediction, as a function of Higgs boson mass (middle). The excluded region is 134-156 GeV. Rightmost plot in figure 2 shows the local  $p_0$  value which is the probability that the background fluctuates to the observed number of events or higher. An interesting small  $p_0$  value, corresponding to  $2.1\sigma$ , is observed at 125 GeV. However it is no more significant when the look-elsewhere-effect is considered [7].

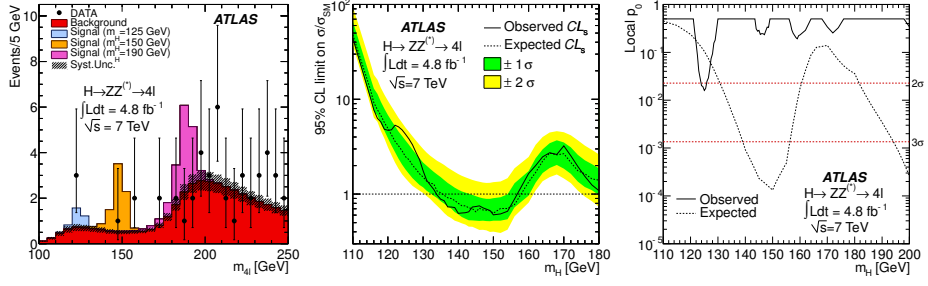


Figure 2: Left:  $m_{4l}$  distribution [7]. Middle: The observed and expected 95% upper limit, divided by the SM prediction, as a function of the Higgs mass. Right: local  $p_0$  as a function of the Higgs mass. The observed local  $p_0$ -value (solid line) and expected median local  $p_0$ -value for the signal hypothesis when tested at  $m_H$  (dashed line).

### 2.3 $H \rightarrow WW \rightarrow l\nu l\nu$ channel

This is the most sensitive channel in the wide mass range of 120-200 GeV. The signal yield is relatively high and the background yield is acceptable thanks to dilepton ( $ee, e\mu$  and  $\mu\mu$ ) plus high missing transverse energy,  $E_T^{miss}$ , requirement. In this analysis, the event selections are optimized according to the presence of jets because the signal and background composition is different depending on jet multiplicity. It is not possible to reconstruct the invariant mass due to two neutrinos in the final state. Hence the transverse mass,  $m_T$ , defined in [8] is used as a final discriminant. Figure 3 shows  $m_T$  distribution and the observed and expected 95% CL upper limit on the cross section, divided by the SM prediction, as a function of the Higgs boson mass. No significant excess is observed [8]. The excluded region is 133-261 GeV.

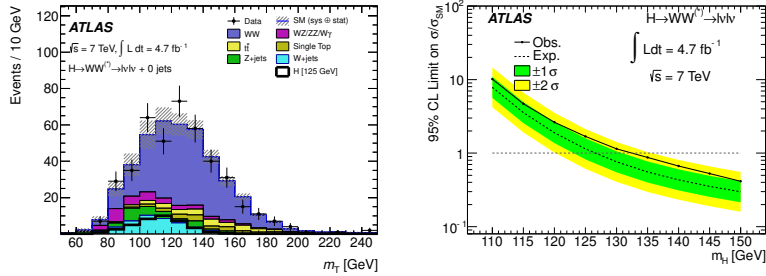


Figure 3: Left:  $m_T$  distribution in 0-jet events [8]. Right: The observed and expected 95% CL upper limit on the cross section, divided by the SM prediction, as a function of the Higgs mass.

## 2.4 $H \rightarrow \tau\tau$ and $H \rightarrow b\bar{b}$ channels

In  $\tau\tau$  channel, two leptonic  $\tau$ , one leptonic  $\tau$  plus one hadronic  $\tau$  and two hadronic  $\tau$  channels are studied separately. Each decay channel is further subdivided into different categories according to the presence of jets. In all channels, no significant excess is observed. Combining all channels, 95% CL upper limit on the cross section is 3.2 times higher than the SM prediction at 125 GeV [9].

In  $b\bar{b}$  channel,  $WH \rightarrow \ell\nu b\bar{b}$ ,  $ZH \rightarrow \ell b\bar{b}$  and  $ZH \rightarrow \nu\nu b\bar{b}$  final states are studied separately. Each final state is subdivided depending on boson momentum,  $p_T^V$ , or  $E_T^{miss}$  to optimize sensitivity because the boosted category with high  $p_T^V$  or high  $E_T^{miss}$  gives better S/B. Combining all channels, 95% CL upper limit on the cross section is 3.5 times higher than the SM prediction at 125 GeV [10].

## 3 Summary

ATLAS has searched for the SM Higgs boson, exploring in particular the low mass region, with the 2011 full data which corresponds to approximately  $5\text{fb}^{-1}$ . Almost all low mass region is excluded except for small region around 125 GeV mass. In particular, for the  $H \rightarrow \gamma\gamma$  and  $ZZ \rightarrow 4\ell$  decay modes about  $2\sigma$  excess in local  $p_0$  is observed around 125 GeV. The excess is consistent with the SM prediction.

## References

- [1] ALEPH, DELPHI, L3 and OPAL Collaborations, Phys. Lett. **B565**, 61 (2003).
- [2] CDF, D0 Collaborations, FERMILAB-CONF-12-065-E.
- [3] ATLAS and CMS collaborations, ATLAS-CONF-2011-157, CMS-PAS-HIG-11-023 (2011). <https://cdsweb.cern.ch/record/1399599>.
- [4] ALEPH, CDF, D0, DELPHI, L3, OPAL, SLD Collaborations, CERN-PH-EP-2010-095, arXiv:1012.2367 [hep-ex], 2010.
- [5] ATLAS Collaboration, 2008 *JINST* **3** S08003.
- [6] ATLAS Collaboration, Phys. Rev. Lett. **108**, 111803 (2012).
- [7] ATLAS Collaboration, Phys. Lett. **B710**, 383-402 (2012).
- [8] ATLAS Collaboration, Phys. Lett. **B716**, 62-81 (2012).
- [9] ATLAS Collaboration, ATLAS-CONF-2012-014, <https://cdsweb.cern.ch/record/1429662>.
- [10] ATLAS Collaboration, ATLAS-CONF-2012-015, <https://cdsweb.cern.ch/record/1429664>.